The Extension of the Hauser-Feshbach Fission Fragment Decay Model to Multi-chance Fission and its Application to ^{239}Pu

LA-UR-22-29923

A. E. Lovell[1], T. Kawano[1], S. Okumura[2], M. R. Mumpower[1], I. Stetcu[1], and P. Talou[1]

[1]Los Alamos National Laboratory, Los Alamos, NM 87545, USA
[2]NAPC–Nuclear Data Section, International Atomic Energy Agency, Vienna A-1400, Austria

Abstract. The Hauser-Feshbach fission fragment decay model, CGMF, calculates the statistical decay of fission fragments through both prompt and delayed neutron and ray emissions in a deterministic manner. While previously limited to the calculation of only first-chance fission, the model has recently been extended to include multi-chance fission, up to neutron incident energies of 20 MeV. The deterministic decay takes as input pre-scission quantities– fission probabilities, pre-fission neutron energies, and the average energy causing fission– and post-scission quantities–yields in mass, charge, total kinetic energy, spin, and parity. From those fission fragment initial conditions, the full decay is followed through both prompt and delayed particle emissions. The evaporation of the prompt neutrons and rays is calculated through the Hauser-Feshbach statistical theory, taking into account the competition between neutron and ray emission, conserving energy, spin, and parity. The delayed emission is taken into account using time-independent calculation using decay data. This whole formulation allows for the calculation of prompt neutron and ray properties, such as multiplicities and energy distributions, both independent and cumulative fission yields, and delayed neutron observables, in a consistent framework. Here, we describe the implementation of multi-chance fission into the CGMF model, and show an example of prompt and delayed quantities beyond first-chance fission, using the example of neutron-induced fission on ^{239}Pu. This expansion represents significant progress in consistently modeling the emission of prompt and delayed particles from fissile systems.

1 Introduction

A great deal of effort has been put into the consistent modeling of the fission process, from the formation of the compound nucleus to the emission of prompt and delayed neutrons and rays. Still, modeling this full process has not yet been accomplished, due to the required computational resources and the accuracy needed for a variety of applications. Various microscopic and microscopic-macroscopic models [1–12] have been used to describe the evolution of the compound nucleus from the saddle point to scission, most being able to calculate some combination of the fission fragment masses, charge, kinetic energies, and excitation energies. However, none of these models are able to then perform the de-excitation of the fission fragments. The consistent emission of prompt neutrons and rays is calculated by several other models, such as BeoH [13, 14], CGMF [15], FREYA [16, 17], FIFRELIN [18], and GEF [19].

To perform these types of consistent calculations, typically, information about the initial conditions of the fission fragments is required—distributions in mass, charge, total kinetic energy, spin, and parity–along with information about the compound nucleus before scission–multi-chance fission probabilities, energies and multiplicities of the neutrons emitted before fission. From there, the models either perform a Monte Carlo sampling of the fission fragment initial conditions and de-excite the fission fragments or deterministically de-excite the fragments. This type of consistent modeling of prompt and delayed neutron and ray observables aims to solve the problem of discrepancies between evaluated quantities [20] caused by the use of independent modeling for quantities that are inherently linked.

In this work, we show results from one such model, BeoH [13, 14]. The required updates to provide prompt and delayed quantities past first-chance fission are reviewed in Sec. 2, and a few results for the case of ^{239}Pu(n,f) are shown in Sec. 3. Finally, we conclude and mention future work in Sec. 4.

2 Theory

The Hauser-Feshbach Fission Fragment Decay (HF)^{3}D model has been updated from the work of Okumura, et al. [13] beyond the calculation of only first-chance fission. Here, we give an overview of the implementation of multi-chance fission; more details can be found in [14]. For the first-chance fission calculation, the determination of the fission fragment initial conditions are straightforward. All possible fission fragment pairs (A_L,Z_L) and (A_H,Z_H)–are constructed and their pre-neutron emission yields are cal-

e-mail: lovell@lanl.gov

culated from joint $Y(A,Z)$ distributions. The pre-neutron emission mass distribution, $Y(A)$, is a sum of three Gaussians, $Y(A) = G_0(A|E_{inc}) + G_2(A|E_{inc}) + G_2(A|E_{inc})$, where G_0 is symmetric about half of the compound mass number ($A_c = 240$ for ^{239}Pu(n,f) in the first-chance energy region) and G_1 and G_2 are asymmetric. The weights, means, and standard deviations of each Gaussian depend on the incident neutron energy. The charge distribution, $Y(Z|A)$, is given by the Wahl systematics [21].

The total kinetic energy, TKE, for each mass is a Gaussian, with a mass-dependent mean and width; the mean is scaled to reproduce the average TKE for the given incident neutron energy. The total excitation energy, TXE, is determined based on the Q value of the specific fission fragment split, TXE = Q − TKE. The excitation energy is shared between the light and heavy fragments based on a ratio of temperatures, R_T, which can be taken to be mass-dependent to better reproduce the average prompt neutron multiplicity as a function of fission fragment mass, $\bar{\nu}_p(A)$. TKE is shared between the two fragments based on kinematics and momentum conservation.

The population of each fragment is constructed as a function of excitation energy, spin, and parity, $P_{l,h}(E_x, J, \pi)$. The fragments are then allowed to de-excite via neutrons and rays using the Hauser-Feshbach statistical theory. The resulting populations of each residual nucleus are collected.

To extend the calculation past first-chance fission, above incident energies of about 5 MeV, further information about the compound nucleus is needed, weighted by the multi-chance fission probabilities. Along with information about the pre-fission neutrons emitted before the compound nucleus fissions, calculations are needed for the excitation energy causing fission and the total kinetic energy at the equivalent incident neutron energy. With the equivalent incident energy and average excitation energy, the pre-neutron emission distributions, $Y(A,Z,TKE,J,\pi)$, are calculated for each compound system that can fission. The Hauser-Feshbach statistical theory is again used to de-excite all of the produced fission fragments.

The prompt observables are calculated as a weighted sum of the results of the Hauser-Feshbach calculation for each fragment. For example, the average prompt neutron multiplicity for each fragment is the integral over the neutron energy spectrum, $\chi(\epsilon)$, $\bar{\nu}_{l,h} = \int \epsilon\,\chi_{l,h}(\epsilon)\,d\epsilon$ for the light, l, and heavy, h, fragments. These average multiplicities get weighted by the pre-neutron emission yields,

$$\bar{\nu}_p = \sum_k [Y_l(k)\bar{\nu}_l + Y_h(k)\bar{\nu}_h] + \sum_{m>0}(m-1)P_f(m). \quad (1)$$

The second term in Eq. (1) takes into account the pre-fission neutron emission, where m is the m^{th} fission chance, and $P_f(m)$ is the multi-chance fission probability of the m^{th} fission chance. In this work, we consider incident energies from thermal to 20 MeV, with $m = 1,2,3,4$. The average prompt-ray multiplicity is calculated in a similar fashion, although there are no pre-fission rays emitted.

At this step in the decay, we have calculated the independent yields and begin to keep track of the isomeric states, M, that are populated. To go from the independent yields, $Y_I(A,Z,M)$, to the cumulative yields, $Y_C(A,Z,M)$, a time-independent calculation is performed,

$$Y_C(A_i,Z_i,M_i) = Y_I(A_i,Z_i,M_i) + \sum_j^N \sum_{\grave{}}^{L_j} Y_C(A_j,Z_j,M_j) b_{j\grave{}\,;i}, \quad (2)$$

where $b_{j\grave{}}$ are the branching ratios with L_j total decay modes, N is the total number of nuclei that produce the i^{th} nucleus, and $_{j\grave{}\,;i}$ connect $Y_C(A_j,Z_j,M_j)$ with $Y_C(A_i,Z_i,M_i)$. The branching ratios are taken from the ENDF/B-VIII.0 [22] decay data library; therefore, when these types of calculations are used to inform the fission product yield evaluations in a future ENDF release, they will also be consistent with the ENDF decay data.

The delayed neutron emission from nuclei where the branching ratio includes a neutron emission mode can be calculated as

$$_{d,i} = Y_C(A_i,Z_i,M_i) b_{i\grave{}}\, f A_{\grave{}} - A_i g. \quad (3)$$

The average delayed neutron multiplicity per fission, $\bar{\nu}_d$, is calculated by summing over all $_{d,i}$.

3 Results

In our initial publication of the multi-chance fission extension of BeoH [14], we only showed results for ^{235}U(n,f), although calculations for other major actinides in the first-chance fission energy range were performed elsewhere [13, 23]. In the present work, we show the application of the multi-chance fission calculation to ^{239}Pu(n,f), for select observables, from thermal incident neutron energies to 20 MeV. We note that although preliminary optimizations have been performed to better reproduce cumulative fission product yield data, there is still room within the model and parameter space to improve the agreement.

The multi-chance fission probabilities, excitation energies for each fission chance, and the energies of the pre-fission neutrons are given by default CGMF calculations [24]. With these values and the preliminary optimizations for $Y(A,Z,TKE,J,\pi)$ and $R_T(A)$ (the details of these optimizations will be discussed in a future publication), we perform BeoH calculations for ^{239}Pu(n,f) from thermal to 20 MeV incident neutron energies. We calculate the average number of prompt rays, $\bar{N}$, as a function of incident neutron energy, which are low compared to the ENDF/B-VIII.0 evaluation. There is a lack of directly measured data for $\bar{N}$ beyond thermal incident energies, and because this information is not included in the optimization procedure, it is not surprising that the calculation is inconsistent. Additionally, when we compare the prompt fission-ray spectrum, PFGS, across incident energies, we see that the tail of the PFGS increases with the incident neutron energy, as was shown in [14].

In Fig. 1, we show the average prompt and delayed neutron multiplicities, $\bar{\nu}_p$ and $\bar{\nu}_d$ respectively calculated by BeoH compared to experimental data. For both observables, we see reasonable agreement between BeoH and the experimental data across the range of incident energies

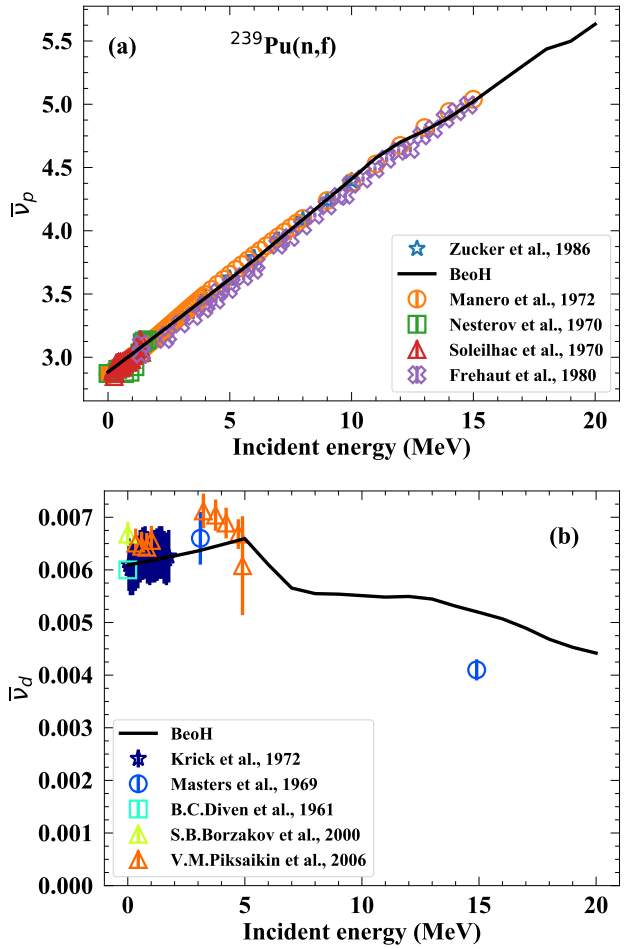

Figure 1. (a) Prompt and (b) delayed average neutron multiplicity for ^{239}Pu(n,f), comparison between BeoH (black solid line) and experimental data (colored, open symbols).

considered here. We also see signs of multi-chance fission where the slopes of $\bar{\nu}_p$ and $\bar{\nu}_d$ change, a result of the change of the compound nucleus that is undergoing fission. For $\bar{\nu}_d$ in particular, we see a strong change in slope after 5 MeV incident neutron energy, due to the opening of second-chance fission. The change in shape of $\bar{\nu}_d$ can also be influenced by the odd-even staggering of the Wahl systematics, as discussed in [23].

Consistently with prompt and delayed neutron and γ-ray observables, we also calculate the fission product yields. In Fig. 2, we show cumulative fission product yields for a handful of isotopes as a function of incident energy, again from thermal to 20 MeV. We see reasonable agreement between the experimental data and BeoH calculations, although we note that ^{99}Mo, panel (c), has a slightly positive slope compared to the at representation in most evaluation, e.g. ENDF/B-VIII.0 [22], and ^{147}Nd, panel (f), has a more shallow slope than the data of Gooden, et al. [25]. Additionally, as with $\bar{\nu}_p$ and $\bar{\nu}_d$, we see clear shape changes in the cumulative fission product yields as a function of incident neutron energy where the multi-chance fission channels open.

4 Conclusions

In this contribution, we have given a brief overview of the extension of the Hauser-Feshbach Fission Fragment Decay (HF^{3}D) Model, BeoH, from a first-chance fission only calculation to being able to take multi-chance fission into account. The extension is shown in more detail using ^{235}U(n,f) as an example in [14], but here, we present the application to neutron-induced fission on ^{239}Pu. The framework allows for the consistent calculation of both prompt and delayed observables as a function of incident neutron energy from thermal to 20 MeV–along with spontaneous fission, although that case was not discussed here. Parametrizations for the initial conditions in mass, charge, total kinetic energy, spin, and parity are constructed for the compound nuclei ^{240}Pu, ^{239}Pu, ^{238}Pu, and ^{237}Pu and then weighted according to multi-chance fission probabilities. Our preliminary optimization shows reasonable agreement between the BeoH calculations and available data for prompt and delayed neutrons and cumulative fission product yields. All of these observables show changes in shape at the opening of multi-chance fission channels, consistent with the change in the fissioning compound nucleus. Further optimization will be performed to produce evaluation-quality fission product yields for ^{239}Pu(n,f) and neutron-induced fission on other major actinides. More details about these calculations will be provided in future publications.

This work was performed under the auspice of the U.S. Department of Energy by Los Alamos National Laboratory under Contract 89233218CNA000001 and was supported by the Office of Defense Nuclear Nonproliferation Research & Development (DNN R&D), with partial support from the Nuclear Criticality Safety Program, both funded and managed by the National Nuclear Security Administration for the U.S. Department of Energy.

References

[1] J. Randrup, P. Möller, Phys. Rev. Lett. **106**, 132503 (2011)
[2] N. Schunck, D. Duke, H. Carr, A. Knoll, Phys. Rev. C **90**, 054305 (2014)
[3] P. Möller, T. Ichikawa, Eur. Phys. J. A **51**, 173 (2015)
[4] A. Bulgac, P. Magierski, K.J. Roche, I. Stetcu, Phys. Rev. Lett. **116**, 122504 (2016)
[5] D. Regnier, N. Dubray, N. Schunck, M. Verrière, Phys. Rev. C **93**, 054611 (2016)
[6] A.J. Sierk, Phys. Rev. C **96**, 034603 (2017)
[7] C. Ishizuka, M.D. Usang, F.A. Ivanyuk, J.A. Maruhn, K. Nishio, S. Chiba, Phys. Rev. C **96**, 064616 (2017)
[8] D.E. Ward, B.G. Carlsson, T. Døssing, P. Möller, J. Randrup, S. Åberg, Phys. Rev. C **95**, 024618 (2017)
[9] M. Verriere, N. Schunck, T. Kawano, Phys. Rev. C **100**, 024612 (2019)
[10] M.D. Usang, F.A. Ivanyuk, C. Ishizuka, S. Chiba, Scientific Reports **9**, 1525 (2019)

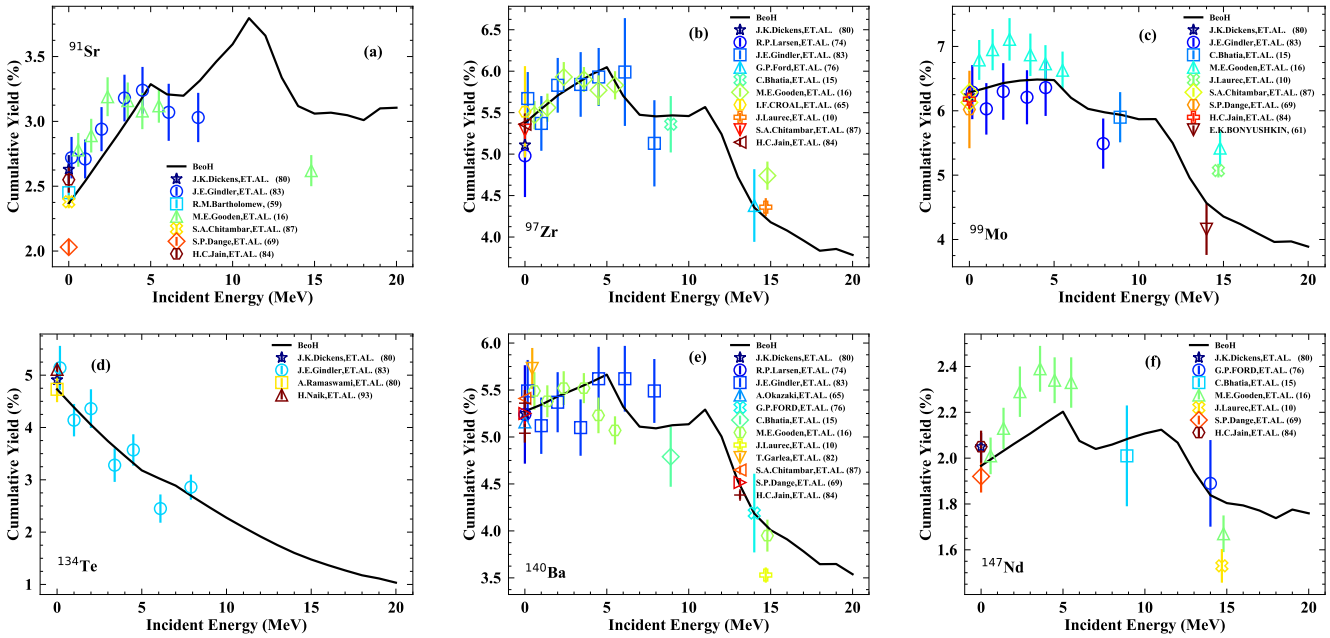

Figure 2. Comparison between BeoH (black solid line) and experimental data (colored, open symbols) for cumulative ssion product yields of ^{239}Pu(n,f), (a) ^{91}Sr, (b) ^{97}Zr, (c) ^{99}Mo, (d) ^{134}Te, (e) ^{140}Ba, and (f) ^{147}Nd.

[11] M. Albertsson, B. Carlsson, T. Døssing, P. Möller, J. Randrup, S. Åberg, Physics Letters **803**, 135276 (2020)
[12] S. Jin, K.J. Roche, I. Stetcu, I. Abdurrahman, A. Bulgac, Computer Physics Communications **269**, 108130 (2021)
[13] S. Okumura, T. Kawano, P. Talou, P. Ja ke, S. Chiba, J. Nucl. Sci. Tech. **55**, 1009 (2018)
[14] A.E. Lovell, T. Kawano, S. Okumura, I. Stetcu, M.R. Mumpower, P. Talou, Phys. Rev. C **103**, 014615 (2021)
[15] P. Talou, I. Stetcu, P. Ja ke, M. Rising, A. Lovell, T. Kawano, Comput. Phys. Commun. **269**, 108087 (2021)
[16] J. Verbeke, J. Randrup, R. Vogt, Computer Physics Communications **191**, 178 (2015)
[17] J. Verbeke, J. Randrup, R. Vogt, Computer Physics Communications **222**, 263 (2018)
[18] O. Litaize, O. Serot, L. Berge, The European Physical Journal A **51**, 177 (2015)
[19] K.H. Schmidt, B. Jurado, C. Amouroux, Tech. Rep. NEA/DB/DOC(2014)1, Nuclear Energy Agency (2014)
[20] P. Ja ke, Nuclear Science and Engineering **190**, 258 (2018), https://doi.org/10.1080/00295639.2018.1429173
[21] A.C. Wahl, Tech. rep., Los Alamos Nat. Lab. LA-13928 (2002)
[22] D. Brown, M. Chadwick, R. Capote, A. Kahler, A. Trkov, M. Herman, A. Sonzogni, Y. Danon, A. Carlson, M. Dunn et al., Nuclear Data Sheets **148**, 1 (2018), special Issue on Nuclear Reaction Data
[23] S. Okumura, T. Kawano, A.E. Lovell, T. Yoshida, Journal of Nuclear Science and Technology **59**, 96 (2022), https://doi.org/10.1080/00223131.2021.1954103
[24] T. Kawano, arXiv:1901.05641v1 (2019)
[25] M. Gooden, C. Arnold, J. Becker, C. Bhatia, M. Bhike, E. Bond, T. Bredeweg, B. Fallin, M. Fowler, C. Howell et al., Nuclear Data Sheets **131**, 319 (2016), special Issue on Nuclear Reaction Data